DOI:10.1021/jf103412d

JOURNAL OF AGRICULTURAL AND FOOD CHEMISTRY
ARTICLE

Granule Structure and Distribution of Allomorphs in C-Type High-Amylose Rice Starch Granule Modified by Antisense RNA Inhibition of Starch Branching Enzyme

Cunxu Wei,[†,‡] Fengling Qin,[†] Weidong Zhou,[§] Huaguang Yu,[§] Bin Xu,[§] Chong Chen,[§] Lijia Zhu,[‡] Youping Wang,[†] Minghong Gu,*[,‡] and Qiaoquan Liu*[,‡]

[†]College of Bioscience and Biotechnology, [‡]Key Laboratories of Crop Genetics and Physiology of the Jiangsu Province and Plant Functional Genomics of the Ministry of Education, and [§]Testing Center, Yangzhou University, Yangzhou 225009, China

C-type starch, which is a combination of both A-type and B-type crystal starch, is usually found in legumes and rhizomes. We have developed a high-amylose transgenic line of rice (TRS) by antisense RNA inhibition of starch branching enzymes. The starch in the endosperm of this TRS was identified as typical C-type crystalline starch, but its fine granular structure and allomorph distribution remained unclear. In this study, we conducted morphological and spectroscopic studies on this TRS starch during acid hydrolysis to determine the distribution of A- and B-type allomorphs. The morphology of starch granules after various durations of acid hydrolysis was compared by optical microscopy, scanning electron microscopy, and transmission electron microscopy. The results showed that amorphous regions were located at the center part of TRS starch subgranules. During acid hydrolysis, starch was degraded from the interior of the subgranule to the outer surface, while the peripheral part of the subgranules and the surrounding band of the starch granule were highly resistant to acid hydrolysis. The spectroscopic changes detected by X-ray powder diffraction, ^{13}C cross-polarization magic-angle spinning NMR, and attenuated total reflectance Fourier transform infrared showed that the A-type allomorph was hydrolyzed more rapidly than the B-type, and that the X-ray diffraction profile gradually changed from a native C-type to a C_B-type with increasing hydrolysis time. Our results showed that, in TRS starch, the A-type allomorph was located around the amorphous region, and was surrounded by the B-type allomorph located in the peripheral region of the subgranules and the surrounding band of the starch granule. Thus, the positions of A- and B-type allomorphs in the TRS C-type starch granule differ markedly from those in C-type legume and rhizome starch.

KEYWORDS: Rice (*Oryza sativa* L.); high-amylose starch granule; C-type starch; allomorph distribution; acid hydrolysis

INTRODUCTION

Storage starch occurs in the form of compact semicrystalline granules and is largely composed of two types of polyglucans: amylopectin and amylose (*1*, *2*). Depending on the botanical source, the starch granule crystallites can adopt two different structures, A- and B-type allomorphs, as revealed by X-ray powder diffraction (XRD). While the A-type allomorph is usually found in starches from cereals and some lower plants, the B-type allomorph occurs in storage organs of dicots (e.g., potato tubers), in some high-amylose starches from cereal mutants (*3*, *4*), and in assimilatory starches from *Solanum tuberosum* L. and *Arabidopsis thaliana* L., etc (*5*). Crystallites are thought to be formed by the clustering of the short lateral chains of amylopectin (*1*). The A-type would occur with short lateral chains and close branching points whereas the B-type is usually formed by amylopectin with long side chains and distant branching points (*1*−*3*). The crystallites are thought to be both made of double helices, but they differ in their unit cells and intracrystalline water contents. The A-type is denser and contains less intracrystalline water than the B-type allomorph. In the B-type allomorph, there is a central water-filled cavity that is surrounded by six double helices (*1*−*3*). Legume and rhizome starches are believed to represent another allomorph, designated as C-type (*6*, *7*). In fact, the C-type allomorph is a mixture of both A- and B-type allomorphs rather than a third distinct type of the double helical arrangement (*6*, *7*).

There have been some studies on the organization and structure of C-type starch granules. For example, in smooth pea starch, the most well-known example of C-type starch, the center of the starch granule consists mainly of the B-type allomorph whereas the A-type allomorph is located toward the outside of the granule (*2*, *6*). Wang et al. (*8*) reported that A- and B-type allomorphs coexisted in individual C-type starch granules of Chinese yam, with the B-type allomorph located at the center

*Corresponding authors. Tel: +86-514-87996648. E-mail: qqliu@yzu.edu.cn (Q.L.), gumh@yzu.edu.cn (M.G.).

 Published on Web 10/29/2010

part of the granule, surrounded by the A-type allomorph at the granule periphery. Recently, we have developed several high-amylose transgenic rice lines (TRS) by antisense RNA inhibition of the starch branching enzymes (*9*, *10*). These transgenic rice grains are rich in resistant starch and have shown significant potential to improve the health of the large bowel in rats (*11*). Our results from microstructure and ultrastructure studies revealed that this high-amylose starch is a semicompound starch granule, which consists of many subgranules surrounded by a continuous band (*10*). Interestingly, the high-amylose rice starch was identified as a C-type crystalline starch by XRD, ^{13}C cross-polarization magic-angle spinning nuclear magnetic resonance (^{13}C CP/MAS NMR), and attenuated total reflectance Fourier transform infrared (ATR-FTIR) analyses (*12*). However, the distributions of A- and B-type allomorphs in these TRS C-type starch granules remained unclear.

Acid modification can change the morphological and gelatinization properties of starch (*13*, *14*), but it does not change the crystalline characteristics of A-type and B-type starches (*15*, *16*). Therefore, acid treatment is very helpful for understanding the internal structure of the starch granule, especially that of the C-type starch (*8*). In this study, the granule structure and distribution of allomorphs in the C-type high-amylose rice starch granule were investigated during acid hydrolysis by a combination of morphological and spectroscopic analyses. The results showed that A- and B-type allomorphs coexisted in each individual C-type starch granule. Amorphous starch was located at the center of the subgranule of the C-type rice starch granule, and this central region was surrounded by the A-type allomorph and then by the B-type allomorph. These results add to our understanding of the allomorph distribution in granules of high-amylose C-type starch and tentatively explain why high-amylose starch is resistant to acid hydrolysis.

MATERIALS AND METHODS

Plant Materials. A transgenic rice line (TRS) with high amylose and resistant starch contents was used in this study. This line was generated from an *indica* rice cultivar Te-qing (TQ) after transgenic inhibition of two starch branching enzymes (SBEI and SBEIIb) through an antisense RNA technique, and is homozygous for the transgene (*9*). The transgenic line (T8 generation) was cultivated in the experimental field of Yangzhou University, Yangzhou, China, in 2009, and its mature grains were used for isolation of starch granules.

Preparation of Starch Samples. Native starch granules were isolated from mature TRS grains, and the acid-modified starches were subsequently prepared from the native starch as described previously (*12*).

Specimen Preparation for Optical Microscopy (OM) and Transmission Electron Microscopy (TEM). The periodic acid−thiosemicarbazide−silver reaction (PATAg) method has been used successfully for TEM investigation of starch granule ultrastructure. Heavy metal ions (silver) can bind to starch molecules after specific oxidation (by periodic acid) of α-glycols at C2−C3 of the starch anhydro-glucose units. Subsequent fixation with thiosemicarbazide results in a high contrast of ultrathin sections of granules under TEM. Since oxidation is more efficient in the starch amorphous regions, the silver ions preferentially bind to the amorphous regions of oxidized starch granules, resulting in dark regions in TEM images, while semicrystalline regions appear lighter (*1*, *17*). Two methods of specimen preparation were used: first, the PATAg method was used to reveal the ultrastructure of native starch granules according to the technique previously described by Li et al. (*17*). However, the acid-modified starch was degraded by periodic acid during specimen preparation with the PATAg method, and therefore, the potassium permanganate ($KMnO_4$) fixation method was used to reveal the internal structure of acid-modified starch for TEM and OM. For $KMnO_4$ fixation, samples were preembedded in an aqueous solution of 3% (w/v) low-melting-temperature agar, the agar was cut into small cubes, and then samples were fixed, dehydrated, and embedded following the method of Wei et al. (*10*). The embedded sample blocks were randomly cut into 1 μm semithin sections with a glass knife on a Leica ultrathin microtome (EM UC6). The semithin sections were stained with periodic acid−Schiff (PAS) reagent, and then observed and photographed with an Olympus BH2 microscope. The ultrathin sections (100 nm thickness) were prepared with a diamond knife on a Leica ultrathin microtome and visualized and photographed with a Philips Tecnai 12 TEM at 100 kV after poststaining with uranyl acetate and lead citrate. For the PATAg method, the ultrathin sections were observed and photographed without poststaining.

Specimen Preparation for Scanning Electron Microscopy (SEM). Native and acid-modified starch samples were suspended in anhydrous ethanol to obtain a 1% (w/v) suspension. One drop of the starch−ethanol suspension was applied to an aluminum stub using double-sided adhesive tape, and the starch was coated with gold before viewing with an environmental SEM (Philips XL-30) at an accelerating voltage of 20 kV.

XRD Analysis. XRD analysis of starch granules was carried out on an X-ray powder diffractometer (D8, Bruker, Germany) as described previously (*12*). All the specimens were stored in a desiccator in which a saturated solution of NaCl maintained the atmosphere at a constant humidity (relative humidity (RH) = 75%). Samples were stored in this way for several days or weeks at 25 °C before measurements. Water contents of the hydrated starch samples were calculated from the weight difference before and after drying at 130 °C. The moisture contents of the hydrated starch samples were approximately 20%. The degree of crystallinity of samples was quantitatively estimated following the method of Nara and Komiya (*18*) with a minor modification. A smooth curve that connected peak baselines was computer-plotted on the diffractogram. The area of peaks at 5.6°, 15°, 17°, 18°, 20° and 23° at 2θ above the smooth curve was taken as the crystalline portion, and the lower area between the smooth curve and a linear baseline that connected the two points of intensity at 2θ of 30° and 4° in the samples was taken as the amorphous section. The upper diffraction peak area and total diffraction area over the diffraction angle 4−30° at 2θ were integrated using JEDA-801D morphological image analysis software (Jiangsu JEDA Science-Technology Development Co., Ltd., Nanjing, China). The ratio of upper area to total diffraction area was taken as the degree of crystallinity.

Solid-state ^{13}C CP/MAS NMR Analysis. Amorphous starch was prepared by gelatinizing native starch following the method of Atichokudomchai et al. (*19*). A 6% (w/v) of TRS starch suspension was heated from 25 to 95 °C at a rate of 1.5 °C/min, held at 95 °C for 15 min and then cooled to 50 °C at a rate of 1.5 °C/min. The starch suspension was spread to form a thin layer before drying overnight in an oven at 60 °C. The amorphous starch sample was blended and sieved through a 100-mesh filter to obtain the amorphous starch powder. High-resolution solid-state ^{13}C CP/MAS NMR analyses of amorphous starch, native starch, and acid modified starch were carried out at B_0 = 9.4 T on a Bruker AVANCE III 400 WB spectrometer. The corresponding ^{13}C resonance frequencies were 100.6 MHz. Samples were packed in a 7 mm ZrO_2 rotor and spun at the magic angle (54.7°) at a spin rate of 6 kHz. ^{1}H−^{13}C CP/MAS spectra were recorded with a contact time of 1.2 ms and a recycle delay of 2 s. The chemical shifts were referenced to tetramethylsilane (TMS) at 0 ppm. Typically, 8000 to 12000 transients were accumulated for the ^{13}C spectra. Before measurements, all specimens were stored for 1 week at 25 °C in a desiccator in which a saturated solution of NaCl maintained the atmosphere at a constant humidity (RH = 75%).

ATR-FTIR Measurement. ATR-FTIR measurement of native and acid-modified starch granules was carried out as described previously (*12*) with a slight modification. The assumed line shape was Lorentzian with a half-width of 19 cm^{-1} and a resolution enhancement factor of 1.9.

RESULTS AND ANALYSIS

Surface Morphological Changes of C-Type TRS Starch Granules during Acid Hydrolysis. SEM micrographs of TRS starch granules before and after acid modification for various periods of time are shown in **Figure 1**. As found previously (*10*), the native TRS starch granules were large and voluminous, and their surfaces showed irregular undulations and/or protrusions of various shapes and sizes, with no evidence of indentations, fissures or pores (**Figure 1A**). In some mechanically cracked starch granules, many polygonal starch subgranules with no indentations were observed. These subgranules located at the periphery of starch

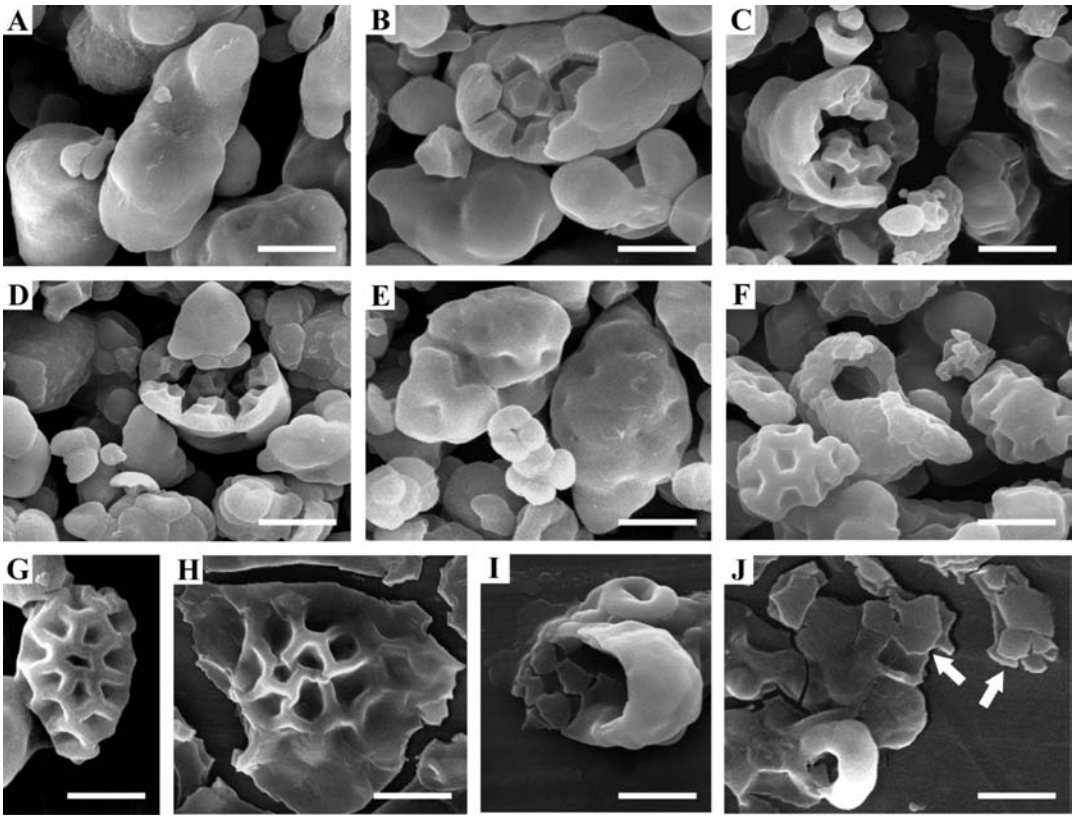

Figure 1. SEM micrographs of native and acid-modified starch granules: (**A**, **B**) native starch; (**C**−**J**) starch modified by acid hydrolysis for 4 days (**C**), 6 days (**D**), 8 days (**E**), 10 days (**F**), 12 days (**G**), 14 days (**H**), 17 days (**I**), and 20 days (**J**). Arrows show broken pieces of acid-modified hollow starch granule. Scale bar = 5 μm.

granules were fused to each other, and adjacent subgranules formed a thick band or wall encircling the entire circumference of each granule (**Figure 1B**).

After 1 and 2 days of acid hydrolysis, the morphology of TRS starch granules and subgranules was similar to that of native starch (data not shown). After acid hydrolysis for 4 days, indentations appeared on the surface of subgranules inside the granule, but the outside surface of whole starch granules remained smooth (**Figure 1C**). After 6 days of hydrolysis, there were more indentations on the surfaces of inner subgranules, but the surface of the whole granule remained smooth without obvious indentations (**Figure 1D**). Indentations were observed on the surface of the starch granules at 8 days of acid hydrolysis (**Figure 1E**). At 10 days of hydrolysis, the cavity was clearly visible within some cracked starch granules, indicating that the interior of the starch granules was essentially hollow (**Figure 1F**). At 12 days of hydrolysis, the surface of the starch granule had severe indentations (**Figure 1G**), and entire starch granules were fractured due to extended indentation after two more days of acid treatment (**Figure 1H**). Cavities were observed in the center of cracked granules (**Figure 1I**), indicating that the interior of starch granules was essentially hollow before they were fractured. After 20 days of hydrolysis, starch granules ruptured and broke into pieces (**Figure 1J**).

Internal Structure of Native and Acid-Modified Starches. TEM micrographs of ultrathin sections of TQ and TRS native starch granule treated with PATAg are shown in **Figure 2**. The TQ native starch subgranule showed a polygonal shape (**Figure 2A**) as reported by Wei et al. (*10*). Many channels (**Figure 2B**) and the alternating amorphous and crystalline lamellar organization of starch (**Figure 2C**) were observed. However, these features were not visible in the ultrathin sections of samples prepared using the potassium permanganate fixation method (*10*). This indicated that the PATAg method was successful for investigating the fine internal structure of starch granules (*1*, *17*). Most of the TRS native starch granules consisted of smaller, packed subgranules that were surrounded by a continuous band. These starch granules were identified as semicompound starch according to our previous results (*10*). This semicompound starch structure of TRS was again confirmed by the PATAg method (**Figure 2D**,**E**). There were three distinct inner structural features of the starch subgranule: the center region, the middle region, and the peripheral region (**Figure 2D**,**E**). The dark center region was the starch amorphous region. The peripheral region of the subgranule was approximately 0.2 μm thick. The middle region lay between the center and peripheral regions (**Figure 2E**).

The ultrastructure of acid-modified starches as determined by the $KMnO_4$ fixation method is presented in **Figure 3**. After 2 days of acid hydrolysis, the center and the middle regions of the starch subgranule were difficult to distinguish, but the appearance of the peripheral region clearly differed from that of the center and middle regions (**Figure 3A**,**D**). After 8 days of acid hydrolysis, the center region and part of the middle region were degraded (**Figure 3B**,**E**). The dark peripheral region narrowed with increasing duration of acid treatment (**Figure 3C**,**F**). After 20 days of hydrolysis, the surrounding band of the starch granules and the narrow peripheral parts of subgranules were clearly observed, indicating that these parts of the starch granules were resistant to acid hydrolysis (**Figure 3G**−**I**). In addition, the internal filamentous structure of starch subgranule could also be observed (**Figure 3G**−**I**). On the surrounding band of the starch granules, there were indentations that may have resulted from the hollow interior of subgranules (**Figure 3G**).

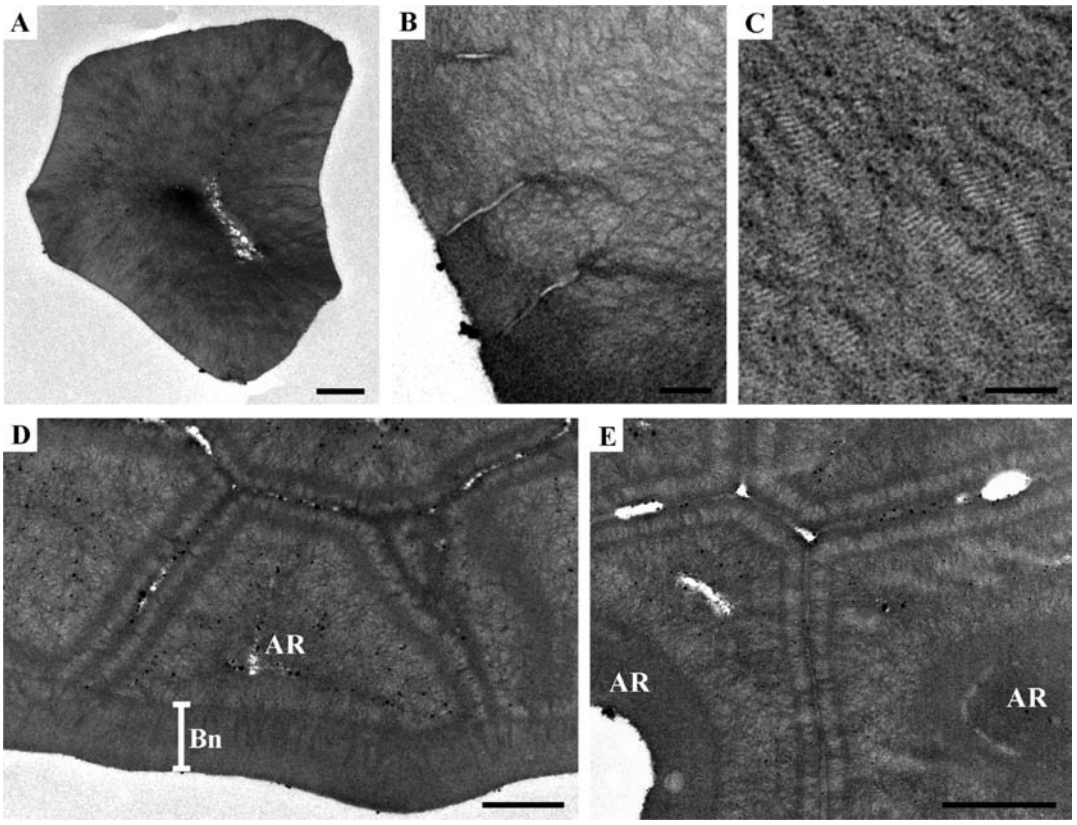

Figure 2. TEM micrographs of native starch granules treated with PATAg: (**A**−**C**) TQ; (**D**) and (**E**) TRS. Bn, continuous band; AR, amorphous region. Scale bar =1 μm for **A**, **D**, and **E**, 200 nm for **B**, and 100 nm for **C**.

We used PAS staining to mark carbohydrates. Semithin sections of native and acid-modified starch granules, prepared using the $KMnO_4$ fixation method, were stained with PAS reagent. The internal microstructural changes are shown in **Figure 4A**. Native TRS starch was not degraded by acid, so the sections were stained so deeply that the profile of subgranules could not be observed (**Figure 4A**,**a**). After 1 or 2 days of acid hydrolysis, the interior of the starch subgranule was lightly stained, and the profile of the subgranules became apparent (**Figure 4A**,**b**). This result implied that some starch component was degraded in the interior of the starch subgranule. Starch components inside the subgranule were gradually degraded with increasing hydrolysis time, and the interior of the subgranule became so lightly stained that the profile of the subgranule became clearer (**Figure 4A**,**c**,**d**). After 8 days of hydrolysis, the interior region of the subgranule showed no staining at all (**Figure 4A**,**e**), indicating that most of the subgranule interior was hollow because most of the starch had been hydrolyzed. After 17 days of hydrolysis, only the peripheral part of the subgranules and the surrounding band of the starch granule were not degraded (**Figure 4A**,**f**). Based on the morphologies of starch granules in **Figure 4A**, starch granules were classified into six types: a-, b-, c-, d-, e-, and f-type, which correspond to the images of starch granule morphologies of **a**, **b**, **c**, **d**, **e**, and **f** in **Figure 4A**. We statistically analyzed the data of percentage of the six types of starch granules during acid hydrolysis (**Figure 4B**). These analyses showed that starch was degraded from the interior of the subgranule to the outer surface, and that some cavities formed at the interior of the starch granule with increasing acid hydrolysis time. The statistical analyses also confirmed that the periphery of the subgranule and the surrounding band of the starch granule were highly resistant to acid hydrolysis.

Crystalline Changes during Acid Hydrolysis. Our previous data from XRD analysis revealed that the C-type crystal of TRS starch changed to B-type during acid hydrolysis (*12*). Hydration induces an increase in degree of granule crystallinity, but does not cause a transition of crystal type (*3*). We used starch samples with almost identical moisture contents (approximately 20%) to minimize the effect of different moisture contents on crystallinity. The XRD patterns of these starches are shown in **Figure 5A**, and the calculated degrees of crystallinity are shown in **Figure 5B**. After 1 day of acid hydrolysis, the TRS starch was still C-type, but the degree of crystallinity significantly increased when compared with that of native starch (**Figure 5**). This may have been due to rapid hydrolysis of amorphous starch at the beginning of acid treatment. At the beginning, XRD shows a mixture between A and B-type allomorphs. Then, the broad peak at 2θ 23° does not exist. In this case, we have a convolution between 3 peaks: 22, 23, and 24°. When part of A-type allomorphs is degraded, the peak at 2θ 23° (A-type peak) is reduced and B-type peaks 22 and 24° become evident. This indicated that the starch crystalline changed from C-type to C_B-type (a C-type closer to B-type) (**Figure 5A**). These results implied that the A-type allomorph in the C-type TRS starch granule was degraded more rapidly than the B-type allomorph during 2−6 days of acid hydrolysis. After 2 days of hydrolysis, the degree of crystallinity gradually increased with increasing hydrolysis time (**Figure 5B**).

Differences of Solid-State NMR Spectra between Native and Acid-Modified Starches. The solid-state ^{13}C CP/MAS NMR spectra of amorphous, native, and acid-modified TRS starches at various times of acid hydrolysis are shown in **Figure 6**. Signals at 94−105 ppm and 58−65 ppm are attributed to C1 and C6 in hexapyranoses, respectively, and the overlapping signal around 68−78 ppm is associated with C2, C3, and C5. According to reports in the literature (*20*, *21*), the two broad shoulders that

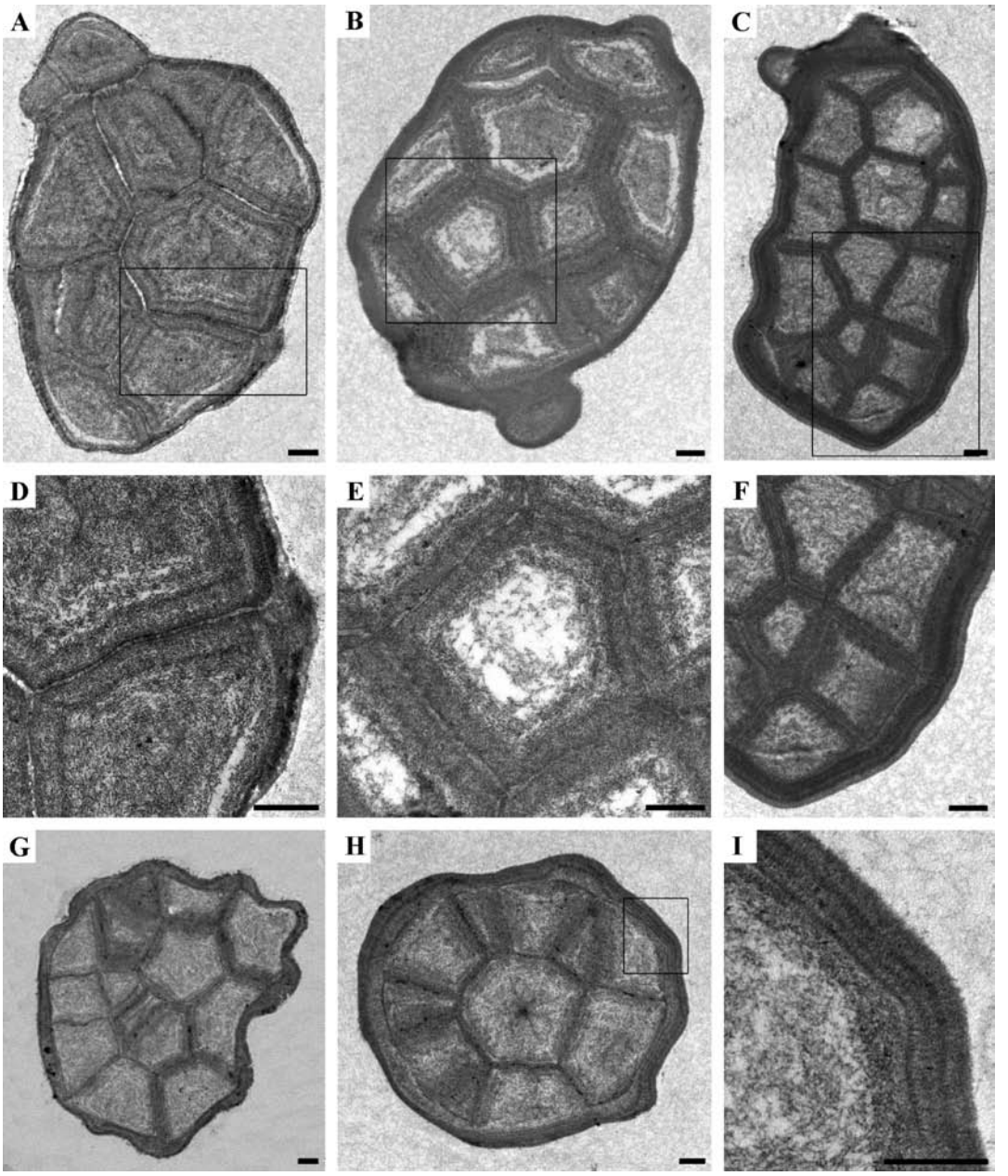

Figure 3. TEM micrographs of acid-modified starch granules prepared using the $KMnO_4$ fixation method: starch modified by acid hydrolysis for 2 days (**A**, **D**), 8 days (**B**, **E**), 14 days (**C**, **F**), and 20 days (**G**, **H**, **I**). (**D**, **E**, **F**, and **I**) Magnification of square in **A**, **B**, **C**, and **H**, respectively. Scale bar = 2 μm.

appeared at 103 and 95 ppm can arise from the amorphous domains for C1, and another broad resonance at 82 ppm can appear from the amorphous domains for C4. These broad resonances were absent from the A- and B-type spherulitic crystal spectra, but were dominant in spectra from amorphous samples (*22*) (**Figure 6**).

There were remarkable differences in the ^{13}C CP/MAS NMR spectra between nontreated native TRS starch and acid-modified starches (**Figure 6**). First, the inconspicuous triplets of C1, especially the weak peak at 101.4 ppm, indicated that A-type allomorph was predominant in native C-type TRS starch. In acid-modified starches, however, the characteristic doublet of C1 for B-type crystalline indicated that the B-type allomorph was dominant.

Second, the intensity of C1 and C4 amorphous resonance decreased with increasing hydrolysis time, and almost disappeared after 17 days of hydrolysis. As well, the NMR spectra of acid-treated starches showed a sharper shape than spectra of native starch. In general, amorphous compounds give broad resonances, because the distribution of local molecular environments gives rise to a broad distribution of chemical shifts for each carbon. On the contrary, ordered materials always show narrower resonances due to the higher regularity of the environment (*22*, *23*). Therefore, the dramatic sharpening of ^{13}C CP/MAS NMR spectra during acid hydrolysis demonstrated the decrease of amorphous starch in TRS starch granules. This indicates that amorphous starch was hydrolyzed more rapidly than crystalline starch.

The last notable difference was the resonance change for C-2, C-3, and C-5 during acid hydrolysis, i.e., the overlapping strong signal around 68−78 ppm associated with C-2, C-3, and C-5 split into two well-resolved signals during acid treatment.

The above three differences in the ^{13}C CP/MAS NMR patterns between native and acid-modified starches revealed two important facts about the structural changes during acid hydrolysis: (1) the amorphous starch in the starch granules was hydrolyzed more

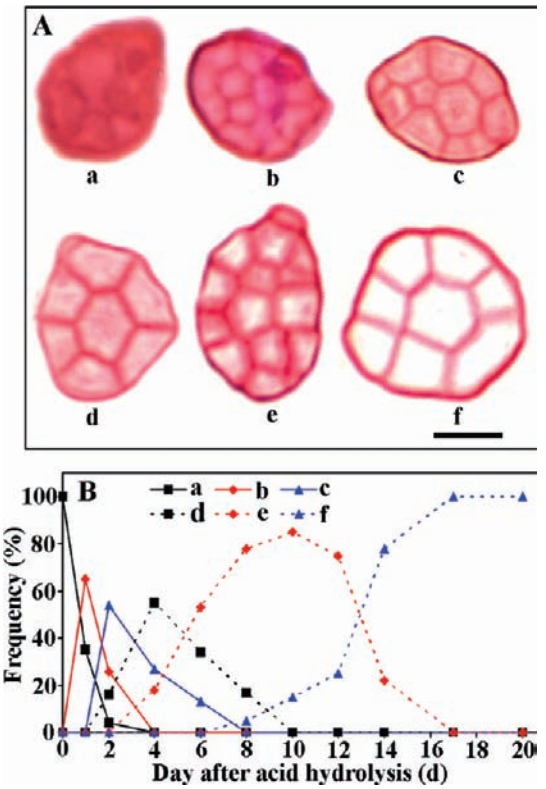

Figure 4. OM micrographs and percentage of native and acid-modified starch granules stained with PAS reagent. (**A**) OM micrographs: (**a**) native starch; (**b**−**f**) starch modified by acid hydrolysis for 1 day (**b**), 2 days (**c**), 4 days (**d**), 8 days (**e**), and 17 days (**f**). Scale bar = 10 μm. (**B**) Percentage of types of acid-modified starch granules. a-, b-, c-, d-, e-, and f-type starch granules correspond to the images of **a**, **b**, **c**, **d**, **e**, and **f** starch granule morphologies in panel **A**. More than 100 starch granules from stained semithin sections were observed at different times of acid hydrolysis.

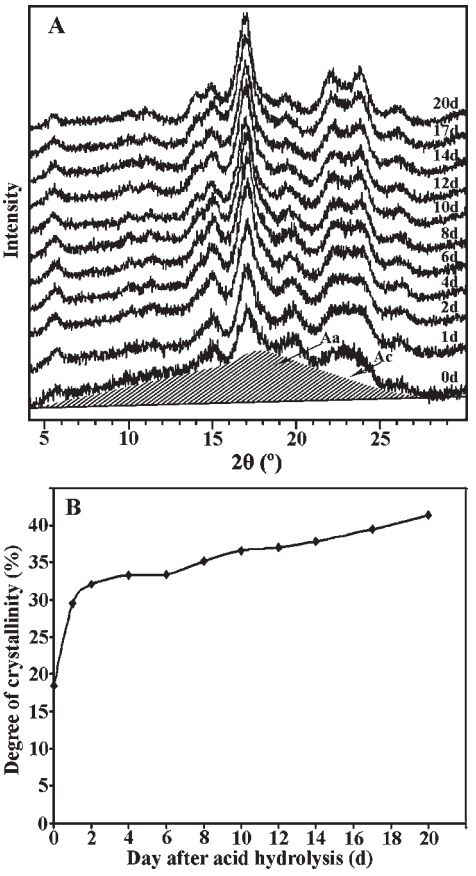

Figure 5. XRD spectra and the degree of crystallinity of native and acid-modified starches. (**A**) XRD spectra. Aa and Ac refer to amorphous and crystallized areas, respectively, on XRD spectra. (**B**) Degree of crystallinity.

rapidly than the crystalline starch; and (2) the A-type allomorph in the C-type starch granules was degraded faster than the B-type.

Difference of ATR-FTIR Spectra between Native and Acid-Modified Starches. Infrared spectroscopy, which detects interactions at the local-range order, has already been used to describe the organization and structure of starch, and the bands at 1045 and 1022 cm^{-1} have been linked with ordered/crystalline and amorphous regions in starch, respectively (*24*). The ratio of absorbance at 1045 and 1022 cm^{-1} was used to quantify the degree of order in starch samples. Intensity ratios of 1045/1022 and 1022/995 cm^{-1} might, therefore, be useful as a convenient index of FTIR data in comparison with other measures of starch conformation (*25*). **Figure 7** shows the original and deconvoluted ATR-FTIR spectra in the region of 1200−900 cm^{-1} of native and acid-modified starch samples. The relative intensities of FTIR bands at 1045, 1022, and 995 cm^{-1} were recorded from the baseline to peak height and the ratios for 1045/1022 and 1022/995 cm^{-1} were calculated as in **Figure 7**. Two remarkable differences were observed. First, the intensity of the band at 1022 cm^{-1} rapidly decreased from 1 to 4 days of acid hydrolysis, and then slowly decreased thereafter. Second, the IR ratios of 1045/1022 cm^{-1} increased with increasing time of acid hydrolysis. These results provided further evidence that the amorphous starch in the C-type starch granule was hydrolyzed first during acid treatment.

DISCUSSION

In plants, starch granule growth originates from the hilum (*26*). The region around the hilum is known as the central region, which consists of amorphous starch. In nonwaxy starches, the central region contains both linear amylose and branched amylopectin, but the central region of waxy starches contains only amylopectin (*17*, *27*, *28*). The central amorphous starch region is larger in high-amylose starch (*17*). In our high-amylose TRS endosperm, the semicompound starch granule consists of many subgranules surrounded by a continuous band, and the central region of TRS starch subgranules is rich in amylose (*10*).

The pattern of degradation of the starch granule during acid hydrolysis can reveal much information about the internal structure of starch granules (*13*−*16*, *29*). In general, there are two phases that can be distinguished during acid hydrolysis of starch. The first phase consists of the relatively fast hydrolysis of amorphous central regions, while the second phase is the slow hydrolysis of the crystalline regions (*30*, *31*). In the studies of Wang et al. (*7*, *8*), morphological studies by SEM showed that the amorphous region was located at the center of C-type starch granules, and that this region was preferentially degraded during acid hydrolysis. Some concave areas appeared on the surface of acid-modified starch granules with increasing hydrolysis time, suggesting that the interior of starch granule was essentially hollow after hydrolysis (*7*, *8*). In this study, we also observed some concave regions on the surfaces of acid-modified starch subgranules and starch granules, but their internal structures were still unclear in SEM micrographs (**Figure 1**). To observe the changes of internal structure of acid-modified starch granules, we used OM and TEM to identify the internal structure during acid hydrolysis of starch granules. The results clearly showed that, during acid hydrolysis, the central region of the TRS starch subgranule was hydrolyzed to form a cavity, but the peripheral

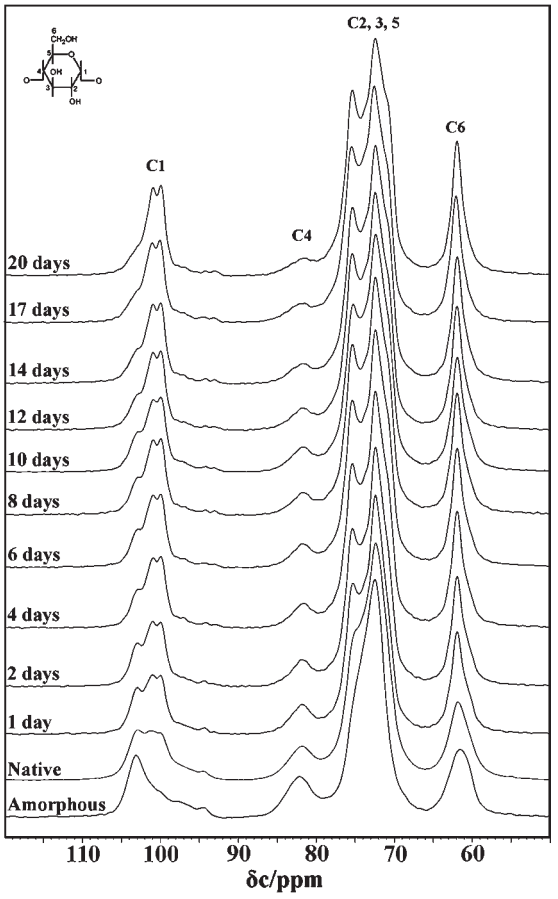

Figure 6. ^{13}C CP/MAS NMR spectra of native and acid-modified starches.

part of the subgranule and the surrounding band of the starch granule remained intact, showing high resistance to acid hydrolysis.

In the present study, during or after acid treatment of TRS native starch, the amount of A-type allomorphs is reduced but the C-type profile is still recognized since the XRD data is of low quality (high level of noise) and the 2θ 5.6° peak which is typical for B-type starches is not as clear as it should be. These phenomena indicated that the crystal type of TRS starch changed from a typical C-type to the C_B-type after acid modification. This result differs from those reported elsewhere (*8*, *16*, *32*); for example, acid-modified corn starches show the same crystalline type as their native starch (*16*), while the crystal type of pea and Chinese yam starches changes from C-type to A-type after acid hydrolysis (*8*, *32*). This fact that our TRS starch changed from C- to C_B-type during acid treatment may be because the A-type crystalline starch degraded faster than B-type starch. After 1 day of acid hydrolysis, the degree of crystallinity calculated from XRD patterns significantly increased compared with that of native starch (29.5% vs 18.5%) and then slowly increased with increasing acid hydrolysis time. This result indicates that the amorphous regions were hydrolyzed first, which agrees with the conclusions of previous studies (*7*, *8*, *19*, *24*) and was further confirmed by ^{13}C CP/MAS NMR and ATR-FTIR analyses. The intensity of C1 and C4 amorphous resonances from the ^{13}C CP/MAS NMR of TRS acid starches decreased gradually with increasing acid hydrolysis time, and almost disappeared completely after 20 days of acid hydrolysis. This result also indicated that the amorphous regions in the starch granules were hydrolyzed first, and could be hydrolyzed completely as long as the hydrolysis time was sufficient. This is in agreement with the findings of previous studies (*7*, *8*, *19*). The bands at 1045 and 1022 cm^{-1} of

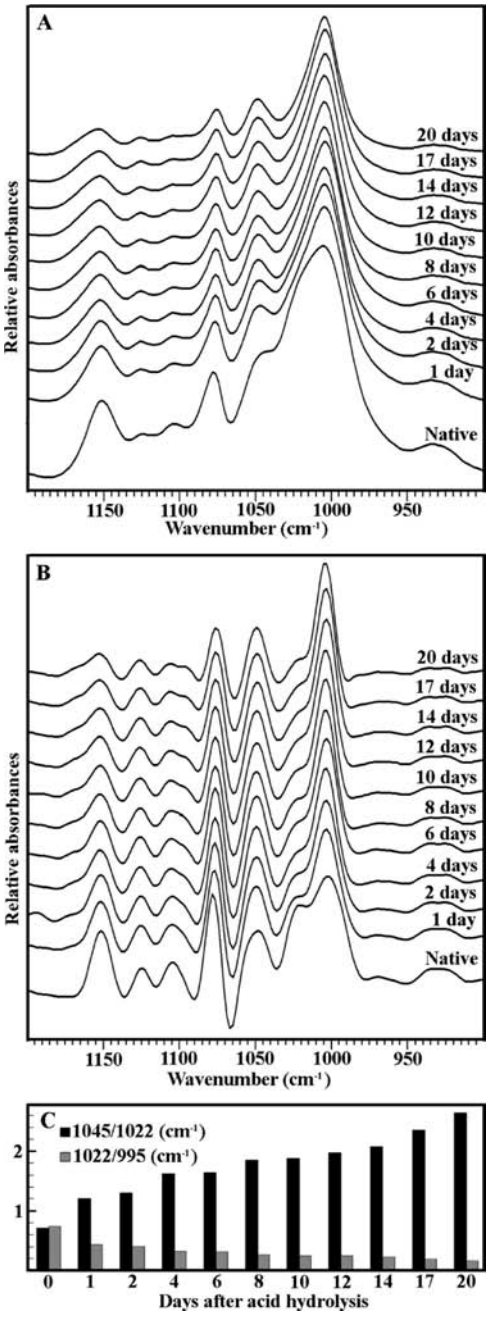

Figure 7. ATR-FTIR spectra of native and acid-modified starches: (**A**) original spectra; (**B**) deconvoluted spectra; (**C**) IR ratio of absorbances 1045/1022 and 1022/995 cm^{-1}.

ATR-FTIR are associated with the ordered/crystalline and amorphous regions in starch, respectively (*24*). The ratio of absorbance 1045/1022 cm^{-1} was used to quantify the degree of order in starch samples (*24*). In the present study, the band at 1022 cm^{-1} was sensitive to acid hydrolysis, whereas the band at 1045 cm^{-1} was not. The intensity of the band at 1022 cm^{-1} decreased with increasing time of acid hydrolysis, which provided further evidence that the amorphous regions in the starch granules were hydrolyzed first.

C-type starch is a combination of A- and B-types, but the distributions of A- and B-allomorphs in C-type cereal starch have not been elucidated. Bogracheva et al. (*6*) used a combination of techniques such as DSC, XRD, and NMR to study the structure of C-type starch from smooth pea seeds. They concluded that C-type starch granules contained both types of polymorph: the

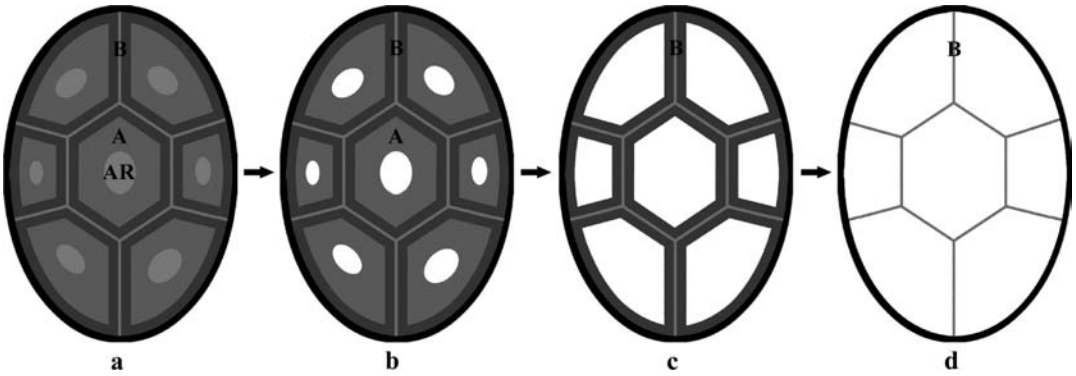

Figure 8. Granule structure model of native and acid-modified starches: (**a**) native starch; (**b**−**d**), acid-modified starches. AR, amorphous regions; A, A-type crystal; B, B-type crystal.

B-type polymorph located in the center, surrounded by the A-type polymorph. Using synchrotron microfocus mapping, Buléon et al. (*2*) observed the same patterns of localization in C-type pea starch. Recently, Wang et al. (2009) reported a similar crystalline microstructure and polymorphism of C-type starch from Chinese yam, and showed that the B-type allomorph was hydrolyzed more rapidly than the A-type (*8*). Thys et al. (2008) studied the effect of alkaline treatment on the ultrastructure of C-type pinhão starch granules (*33*). Their results indicated that the B-type allomorph was partially degraded while the A-type allomorph remained almost intact when granules were alkali-treated. They suggested two possible patterns of allomorph distribution: (1) the B-type allomorph is located at an external region of the starch granule (as determined by the external degradation of the starch granule), or (2) the B-type allomorph is located at the center of the starch granule (as determined by the leaching of amylose from the starch granule caused by the partial alkaline gelatinization promoted by the alkaline solution) (*33*). In the present study, XRD spectra indicated that TRS starch crystal type gradually changed from the native C-type to the C_B-type with increasing acid hydrolysis time. This was mainly because the A-type allomorph degraded more rapidly than the B-type during acid hydrolysis. In the present study, we observed the degradation of TRS starch from the interior of the subgranule to the outer surface by OM, SEM, and TEM. The results of these analyses suggested that the A-type allomorph was distributed at the center of the TRS starch subgranule. This differs to the case of C-type granules from pea and rhizome starches, in which the A-type allomorph is localized in external regions of the granules, while the B-type is localized in the center (*2*, *6*−*8*).

From the results of the ultrastructure of native TRS starch treated with PATAg, and the morphological and spectroscopic changes of acid-modified starches, we proposed a model of TRS granule structure and its change during acid hydrolysis (**Figure 8**). In this model, the amorphous region is located in the core of subgranules of semicompound starch granules from TRS endosperm, the A-type crystalline is located around the amorphous region, and the B-type crystalline is located in the peripheral part of subgranules and in the band that surrounds the semicompound starch granule (**Figure 8a**). The change in the structure of TRS starch granules showed three phases as a function of time during acid hydrolysis. First, the amorphous regions were rapidly hydrolyzed (**Figure 8b**), which resulted in a significant increase in the degree of crystallinity, but no change in the XRD pattern. Then, the A-type crystalline was gradually hydrolyzed (**Figure 8c**), which resulted in the disappearance of the characteristic A-type diffraction peak and the appearance of a typical B-type diffraction peak. Finally, the B-type crystalline was partly hydrolyzed, but the peripheral part of the subgranule and the surrounding band of the starch granule, both of which consisted of the B-type allomorph, remained intact and were highly resistant to acid hydrolysis (**Figure 8d**).

ABBREVIATIONS USED

ATR-FTIR, attenuated total reflectance Fourier transform infrared; ^{13}C CP/MAS NMR, ^{13}C cross-polarization magic-angle spinning nuclear magnetic resonance; OM, optical microscopy; PAS, periodic acid−Schiff; PATAg, periodic acid−thiosemicarbazide−silver reaction; SEM, scanning electron microscopy; TEM, transmission electron microscopy; XRD, X-ray powder diffraction.

LITERATURE CITED

(1) Gallant, D. J.; Bouchet, B.; Baldwin, P. Microscopy of starch: evidence for a new level of granule organization. *Carbohydr. Polym.* **1997**, *32*, 177−191.

(2) Buléon, A.; Gérard, C.; Riekel, C.; Vuong, R.; Chanzy, H. Details of the crystalline ultrastructure of C-starch granules revealed by synchrotron microfocus mapping. *Macromolecules* **1998**, *31*, 6605−6610.

(3) Cheetham, N. W. H.; Tao, L. Variation in crystalline type with amylose content in maize starch granules: an X-ray powder diffraction study. *Carbohydr. Polym.* **1998**, *36*, 277−284.

(4) Kang, H. J.; Hwang, I. K.; Kim, K. S.; Choi, H. C. Comparative structure and physicochemical properties of Ilpumbyeo, a high-quality *japonica* rice, and its mutant, Suweon 464. *J. Agric. Food Chem.* **2003**, *51*, 6598−6603.

(5) Hejazi, M.; Fettke, J.; Haebel, S.; Edner, C.; Paris, O.; Frohberg, C.; Steup, M.; Ritte, G. Glucan, water dikinase phosphorylates crystalline maltodextrins and thereby initiates solubilization. *Plant J.* **2008**, *55*, 323−334.

(6) Bogracheva, T. Y.; Morris, V. J; Ring, S. G.; Hedley, C. L. The granular structure of C-type pea starch and its role in gelatinization. *Biopolymers* **1998**, *45*, 323−332.

(7) Wang, S. J.; Yu, J. L.; Yu, J. G.; Chen, H. X.; Pang, J. P. The effect of acid hydrolysis on morphological and crystalline properties of Rhizoma Dioscorea starch. *Food Hydrocolloids* **2007**, *21*, 1217−1222.

(8) Wang, S. J.; Yu, J. L.; Zhu, Q. H.; Yu, J. G.; Jin, F. M. Granular structure and allomorph position in C-type Chinese yam starch granule revealed by SEM, ^{13}C CP/MAS NMR and XRD. *Food Hydrocolloids* **2009**, *23*, 426−433.

(9) Zhu, L. J. Studies on starch structure and functional properties of high-amylose transgenic rice and different waxy rice varieties. Ph.D. dissertation, Yangzhou University, Yangzhou, China, 2009.

(10) Wei, C. X.; Qin, F. L.; Zhu, L. J.; Zhou, W. D.; Chen, Y. F.; Wang, Y. P.; Gu, M. H.; Liu, Q. Q. Microstructure and ultrastructure of high-amylose rice resistant starch granules modified by antisense

RNA inhibition of starch branching enzyme. *J. Agric. Food Chem.* **2010**, *58*, 1224−1232.
(11) Li, M.; Piao, J. h.; Liu, Q. Q.; Yang, X. G. Effects of the genetically modified rice enriched with resistant starch on large bowel health in rats. *Acta Nutr. Sin.* **2008**, *30*, 588−591.
(12) Wei, C. X.; Xu, B.; Qin, F. L.; Yu, H. G.; Chen, C.; Meng, X. L.; Zhu, L. J.; Wang, Y. P.; Gu, M. H.; Liu, Q. Q. C-type starch from high-amylose rice resistant starch granules modified by antisense RNA inhibition of starch branching enzyme. *J. Agric. Food Chem.* **2010**, *58*, 7383−7388.
(13) Lawal, O. S.; Adebowale, K. O.; Ogunsanwo, B. M.; Barba, L. L.; Ilo, N. S. Oxidized and acid thinned starch derivatitives of hybrid maize: functional characteristics, wide-angle X-ray diffractometry and thermal properties. *Int. J. Biol. Macromol.* **2005**, *35*, 71−79.
(14) Lawal, O. S. Composition, physicochemical properties and retrogradation characteristics of native, oxidised, acetylated and acid-thinned new cocoyam (*Xanthosoma sagittifolium*) starch. *Food Chem.* **2004**, *87*, 208−218.
(15) Wang, L. F.; Wang, Y. J. Structures and physicochemical properties of acid-thinned corn, potato and rice starches. *Starch/Stärke* **2001**, *53*, 570−576.
(16) Wang, Y. J.; Truong, V. D.; Wang, L. F. Structures and rheological properties of corn starch as affected by acid hydrolysis. *Carbohydr. Polym.* **2003**, *52*, 327−333.
(17) Li, J. H.; Vasanthan, T.; Hoover, R.; Rossnagel, B. G. Starch from Hull-less barley: ultrastructure and distribution of granule-bound proteins. *Cereal Chem.* **2003**, *80*, 524−532.
(18) Nara, S.; Komiya, T. Studies on the relationship between water-saturated state and crystallinity by the diffraction method for moistened potato starch. *Starch/Stärke* **1983**, *35*, 407−410.
(19) Atichokudomchai, N.; Varavinit, S.; Chinachoti, P. A study of ordered structure in acid-modified tapioca starch by ^{13}C CP/MAS solid-state NMR. *Carbohydr. Polym.* **2004**, *58*, 383−389.
(20) Cheetham, N. W. H.; Tao, L. Solid state NMR studies on the structural and conformational properties of natural maize starches. *Carbohydr. Polym.* **1998**, *36*, 285−292.
(21) Bogracheva, T. Y.; Wang, Y L.; Hedley, C. L. The effect of water content on the ordered/disordered structures in starches. *Biopolymers* **2001**, *58*, 247−259.
(22) Veregin, R. P.; Fyfe, C. A.; Marchessault, R. H.; Taylor, M. G. Characterization of the crystalline A and B starch polymorphs and investigation of starch crystallization by high resolution ^{13}C CP/MAS NMR. *Macromolecules* **1986**, *19*, 1030−1034.
(23) Paris, M.; Bizot, H.; Emery, J.; Buzare, J. Y.; Buléon, A. Crystallinity and structuring role of water in native and recrystallized starches by ^{13}C CP-MAS NMR spectroscopy: 1: spectral decomposition. *Carbohydr. Polym.* **1999**, *39*, 327−339.
(24) Sevenou, O.; Hill, S. E.; Farhat, I. A.; Mitchell, J. R. Organisation of the external region of the starch granule as determined by infrared spectroscopy. *Int. J. Biol. Macromol.* **2002**, *31*, 79−85.
(25) Htoon, A.; Shrestha, A. K.; Flanagan, B. M.; Lopez-Rubio, A.; Bird, A. R.; Gilbert, E. P.; Gidley, M. J. Effects of processing high amylose maize starches under controlled conditions on structural organization and amylase digestibility. *Carbohydr. Polym.* **2009**, *75*, 236−245.
(26) Shannon, J. C.; Garwood, D. L. Genetics and physiology of starch development. In *Starch: Chemistry and Technology*; Whistler, R. L., Bemiller, J. N., Paschall, E. F., Eds.; Academic Press: New York, 1984; pp 25−86.
(27) Atkin, N. J.; Cheng, S. L.; Abeysekera, R. M.; Robards, A. W. Localisation of amylose and amylopectin in starch granules using enzyme-gold labelling. *Starch/Stärke* **1999**, *51*, 163−172.
(28) Seguchi, M.; Yasui, T.; Hosomi, K.; Imai, T. Study of internal structure of waxy wheat starch granules by KI/I_2 solution. *Cereal Chem.* **2000**, *77*, 339−342.
(29) Sandhu, K. S.; Singh, N.; Lim, S. T. A comparison of native and acid thinned normal and waxy corn starches: physicochemical, thermal, morphological and pasting properties. *LWT—Food Sci. Technol.* **2007**, *40*, 1527−1536.
(30) Kainuma, K.; French, D. Nägeli amylodextrin and its relationship to starch granule structure. I. preparation and properties of amylodextrins from various starch types. *Biopolymers* **1971**, *10*, 1673−1680.
(31) Biliaderis, C. G.; Grant, D.; Vose, J. R. Structural characterization of legume starches. II. studies on acid-treated starches. *Cereal Chem.* **1981**, *58*, 502−507.
(32) Wang, S. J.; Yu, J. L.; Yu, J. G. The semi-crystalline growth rings of C-type pea starch granule revealed by SEM and HR-TEM during acid hydrolysis. *Carbohydr. Polym.* **2008**, *74*, 731−739.
(33) Thys, R. C. S.; Westfahl, H. Jr.; Noreña, C. P. Z.; Marczak, L. D. F.; Silveira, N. P.; Cardoso, M. B. Effect of the alkaline treatment on the ultrastructure of C-type starch granules. *Biomacromolecules* **2008**, *9*, 1894−1901.

Received for review June 24, 2010. Revised manuscript received October 12, 2010. Accepted October 13, 2010. This study was financially supported by grants from the National Natural Science Foundation of China (30828021, 30971754, 31071342), the Ministry of Science and Technology (2009ZX08011-003B, 2008ZX08009-003), the Government of Jiangsu Province (BK2009186), and the China Postdoctoral Science Foundation (20090451252).